ORGANIC PROCESS RESEARCH & DEVELOPMENT
OPR&D
Article
Cite This: Org. Process Res. Dev. 2018, 22, 1365−1372
pubs.acs.org/OPRD

Crystal Structures of Two Important Pharmaceuticals Solved by 3D Precession Electron Diffraction Tomography

Partha P. Das,[†] Enrico Mugnaioli,[‡] Stavros Nicolopoulos,[†] Camilla Tossi,[‡,∥] Mauro Gemmi,[‡] Athanasios Galanis,[†] Gheorghe Borodi,[§] and Mihaela M. Pop*[,⊥]

[†]NanoMegas, Boulevard Edmond Machtens 79, B1080 Brussels, Belgium

[‡]Center for Nanotechnology Innovation@NEST, Istituto Italiano di Tecnologia, Piazza San Silvestro 12, 56127 Pisa, Italy

[§]Molecular and Biomolecular Physics Department, National Institute for R&D of Isotopic and Molecular Technologies, 67-103 Donat, Cluj-Napoca 400293, Romania

[∥]Department of Electronics and Nanoengineering, School of Electrical Engineering, Aalto University, 00076 Aalto, Finland

[⊥]TeraCrystal, 67-103 Donat, Cluj-Napoca 400293, Romania

Supporting Information

ABSTRACT: The crystal structures of two important marketed pharmaceuticals, namely, ramelteon (RAM) and tolvaptan (TOL), were determined for the first time using 3D precession electron diffraction tomography (PEDT) on 500 nm-sized crystals. The results were compared with the same structures determined by single-crystal X-ray diffraction on subsequently grown 50−200 μm single crystals, indicating a good match of molecular conformation, crystal packing, and unit cell parameters. The X-ray crystal structures were used to validate the developed workflow of data acquisition and structure solution with electron diffraction. This study highlights that 3D PEDT alone is able to provide accurate crystal structures from pharmaceutical nanocrystals that will suffice for most practical applications when no larger crystals can be grown.

KEYWORDS: *precession electron diffraction, electron diffraction tomography, crystal structure, ramelteon, tolvaptan*

1. INTRODUCTION

In any program of drug discovery and development, knowledge of the crystal structures of the obtained drug substances is of primary importance for a full understanding of the various types of non-covalent interactions in the solid state and therefore for optimizing the performance of the drugs.[1] Additionally, in the context of drug polymorphism, knowledge of the three-dimensional (3D) fully resolved crystal structure is essential for assessing the polymorphic purity of the drug substance,[2] thereby ensuring reproducibility during scale-up, manufacture, and formulation of the pharmaceutical compounds.[3,4]

Single-crystal X-ray structure analysis currently represents the optimum method for determining the complete structures of crystalline materials.[5] For crystals in the 100−500 μm size range, crystal structure determination by single-crystal X-ray diffraction can be considered a standard procedure, but for smaller crystals, X-ray powder diffraction (XRPD) and NMR crystallography have been the only options.[6−9] However, XRPD may fail in detecting one or more polymorphic modifications associated with nanocrystals, especially if they are present in small amounts (e.g., less than 1−5 wt %) or if the structure of interest is characterized by large cell parameters or pseudosymmetry, causing accidental and systematic overlap of symmetrically independent reflections at medium-high resolution.[10] In fact, XRPD cannot be used for structure determination or refinement of poorly crystalline materials or mixtures of unknown phases or for detection and characterization of minor components in polyphasic samples, components that are often critical for establishing the adequate processing and consistency of the entire material.

Electron diffraction (ED) in a transmission electron microscope (TEM) has a number of important advantages compared with X-ray diffraction. Namely, it allows sampling of much smaller crystals (size range of about 30 nm to several microns) on samples that appear "amorphous" for X-ray diffraction. Structure determinations using ED data are anyway far less frequent, and only recently this has been proved to be a suitable path both for the disclosure of inorganic and organic materials.[11] In the last 10 years, a new technique called automated electron diffraction tomography (ADT or EDT) was developed to collect and process 3D ED data from single nanocrystals.[12,13] EDT is a single-crystal method based on sampling of the reciprocal space in small fixed steps (usually 1° tilt) or by movielike continuous acquisition[14] while the sample is rotated around an arbitrary axis without the need of any prior crystallographic orientation. Compared with traditional ED data acquisitions based on oriented patterns, EDT allows for more complete, less dynamical, and much faster data collection,[15] being in this way suitable also for the characterization of very beam-sensitive materials, like pharmaceuticals. With knowledge of the reciprocal angular step between consecutive patterns, a 3D reciprocal volume can be directly reconstructed, allowing easy cell parameter determination and intensity integration of all reflections present in the covered wedge of reciprocal space.

EDT can be performed in any TEM using a standard single tilt or tomographic holder. The efficiency of the sampling depends on the crystal symmetry: the higher the symmetry, the smaller

Received: May 6, 2018
Published: September 4, 2018

DOI: 10.1021/acs.oprd.8b00149
Org. Process Res. Dev. 2018, 22, 1365−1372

the minimum required angular range. Depending on the different TEM constructions and settings, the available tilt limit is normally between 45° and 70°. A tilt range of 90° (from −45° to +45°) is usually enough for crystal structure determination. However, when a higher tilt range is achieved, a larger portion of the reciprocal space is covered, and this would in turn enhance the accuracy of the structure solution.

The reconstructed diffraction volume may suffer from the acquisition gaps between experimental patterns, which are generally acquired with a fixed tilt step of 1°. Precession electron diffraction (PED)[16,17] can be used to overcome this problem, thereby making ED reflection intensities more suitable for crystal structure determination.[18,19]

Although in the past few years precession electron diffraction tomography (PEDT) has allowed the solution of many complex nanostructures of catalysts,[20,21] metal−organic hybrids,[22,23] minerals,[24,25] intermetallics,[26,27] and other kinds of inorganic compounds,[28,29] there are still a very limited number of examples concerning organic compounds.[30,31] This is mainly due to the high beam sensitivity of these materials and the general need to use TEM cryocooling techniques to slow down the radiation damage.[22,31]

We recently reported the structure determination of two pharmaceutical nanocrystals on the basis of continuous-rotation ED data collected at room temperature using a novel Timepix single-electron direct detection camera.[14,32] In the present work, we expand our investigations to include two complex and marketed pharmaceutical compounds.

Ramelteon (RAM, Figure 1a) was discovered by Takeda Pharmaceutical Company Limited in 1996 and is the first

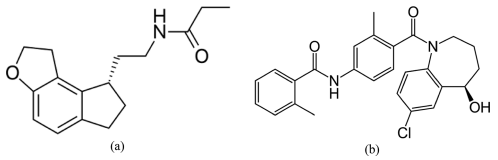

Figure 1. Molecular structures of (a) ramelteon (RAM) and (b) tolvaptan (TOL).

selective melatonin MT_1 and MT_2 receptor agonist approved by the U.S. Food Drug and Administration (FDA) in 2005 for the treatment of insomnia. RAM is the only approved sleep-promoting medication that does not have a direct sedating effect,[33] and recent research has suggested that it might be a candidate for the treatment of recurrent endometrial cancer.[34] The RAM molecule has one chiral center and is produced as the *S* form. The drug substance is a nonhygroscopic crystalline powder, and it has no known polymorphs.[35]

Tolvaptan (TOL, Figure 1b) is a selective, competitive vasopressin receptor 2 antagonist used to treat hyponatremia (low blood sodium levels) associated with congestive heart failure, cirrhosis, and the syndrome of inappropriate antidiuretic hormone (SIADH). TOL has been approved since 2009 in the U.S. and Europe for the treatment of hyponatremia. Since 2015, TOL has become the first pharmaceutical therapy for the treatment of autosomal dominant polycystic kidney disease (ADPKD), being approved in Europe, Canada, and South Korea.[35] The TOL molecule has an asymmetric center and can exist as two enantiomers. Tolvaptan active substance has been developed as a racemate and exhibits no optical rotation. The drug substance is a nonhygroscopic crystalline powder and, like RAM, does not exhibit polymorphism.[36]

Despite their wide use as drugs and lack of polymorphism, the crystal structures of RAM and TOL had not been determined previously (in fact, they are not reported in the Cambridge Structural Database or in the literature).[37,38] In this paper, we report the first crystal structures of RAM and TOL determined by the 3D PEDT technique and compare the results with single-crystal X-ray determinations obtained on subsequently grown single crystals (Table 1). We used the X-ray results to validate the structure solutions obtained by electron diffraction, thereby evaluating the potential of the electron diffraction technique for solving the crystal structures of pharmaceutical compounds.

2. MATERIALS AND METHODS

2.1. Materials and Crystal Growth Experiments. Ramelteon and tolvaptan drug substances were purchased from Afine Chemicals Ltd. as crystalline materials. For the crystal growth experiments, a set of 10 analytical reagent solvents (Tables S1 and S2 in the Supporting Information) were purchased from Merck. Solvent screening experiments were performed by suspending 15−20 mg of drug substance in 1 mL of organic solvent. The samples were heated to 60 °C and then cooled slowly to 15 °C. If suspensions were obtained, the vials were left at room temperature for solvent evaporation, while the solutions were put in the refrigerator at 4 °C in closed vials. For both RAM and TOL, suitable single crystals were obtained from methanol and acetone solutions after 2 days of aging at 4 °C followed by slow evaporation at room temperature.

2.2. TEM Microscopy and 3D Precession Electron Diffraction Tomography. Nanocrystalline dispersions of RAM and TOL samples for TEM observations were obtained by crushing dry crystals into a fine powder between two glass plates. The powder was then sprinkled several times on a holey 300 mesh carbon grid so that a random size distribution of nanocrystals (size about 50−500 nm) could be obtained and transferred on the microscope grid. A Zeiss Libra LaB_6 120 keV microscope equipped with a precession device (Digistar P1000, NanoMEGAS)[39] and scanning TEM (STEM) configuration was used for data collection at the Istituto Italiano di Tecnologia (Pisa, Italy). Low-dose illumination was obtained using a condenser aperture of 5 μm and maintaining a parallel beam illumination with a diameter of about 150 nm on the sample. A novel single-electron Timepix detector (512 × 512 pixels)[40] was used for the PEDT data acquisition.

Several data acquisition methods were tested for both RAM and TOL, which involved stepwise and continuous rotation modes. Stepwise data collection is normally preferred because it ensures a wide angular range by recentering the crystal after every tilt. The drawbacks are that this method is slower than the continuous rotation mode and the crystal suffers a higher dose. While TOL resisted damage for the entire stepwise data collection, RAM revealed more beam sensitivity. As a consequence, the RAM data set was obtained by continuous rotation, even though shorter tilt ranges were covered.

PEDT data were acquired from four RAM crystals (data were collected from crystal areas such as the one indicated in Figure 2) at room temperature in fast continuous mode.[14] The exposure time was kept at 0.5 s, while the rotation speed was changed in order to have tilt series with different angular steps (actually between 0.91° and 1.35°). The precession angle was set at 0.5°. An in-column omega energy filter was used to remove inelastic scattering and enhance the visibility of weak reflections.[56]

DOI: 10.1021/acs.oprd.8b00149
Org. Process Res. Dev. 2018, 22, 1365−1372

Table 1. Crystallographic Data and Details of Crystal Structure Determinations by PEDT and X-ray Crystallography

	RAM		TOL	
	PEDT	X-ray	PEDT	X-ray
formula	$C_{16}H_{21}NO_2$	$C_{16}H_{21}NO_2$	$C_{26}H_{25}ClN_2O_3$	$C_{26}H_{25}ClN_2O_3$
molar mass (g mol^{-1})	259.34	259.34	448.93	448.93
temperature (K)	293	293	93	293
crystal size	200 nm × 200 nm[a]	200 μm × 50 μm × 50 μm	200 nm × 200 nm[a]	100 μm × 100 μm × 40 μm
crystal system	orthorhombic	orthorhombic	monoclinic	monoclinic
space group	$P2_12_12_1$	$P2_12_12_1$	$P2_1/n$	$P2_1/n$
a (Å)	4.99	5.0450(4)	7.52	7.6270(10)
b (Å)	11.92	12.4178(11)	38.53	38.007(4)
c (Å)	22.95	23.187(2)	8.44	8.5629(12)
α (deg)	90	90	90	90
β (deg)	90	90	107.82	108.118(15)
γ (deg)	90	90	90	90
V (Å^3)	1365.08	1452.6(2)	2328.15	2359.1(5)
Z	4	4	4	4
F(000)	560.0	560	940.0	944
calcd density (g/cm^3)	1.262	1.186	1.278	1.264
EDT tilt range (deg)	−55 to +23 −33 to +59 −33 to +71 −48 to +16	–	−40 to +33 −40 to +35 −20 to +38	–
θ range (deg)	–	3.8−70.57	–	4.65−71.35
R_{int} (%)	24.40[c]	2.48	16.55[c]	5.52
% completeness (resolution)	88.2 (1.0 Å)	99.87	64.35 (1.2 Å)	99.35
refined params	–[b]	173	–[b]	296
GOF on F^2	–[b]	1.028	–[b]	1.176
cost function (%)	42.760	–	41.516	–
R_1 (on F, $I > 2\sigma(I)$)	–[b]	0.0672	–[b]	0.0772
wR_2 (on F^2, all data)	–[b]	0.2043	–[b]	0.2528

[a]For PEDT, crystal size refers to the diffracting volume. [b]No least-squares refinement was done for the final SA structure using PEDT data, so values related to the refined parameters, GOF, R_1, and wR_2 are not relevant for this publication. [c]Because of strong dynamical diffraction in PEDT, higher values of R_{int} are observed for the PEDT data compared with the X-ray data.

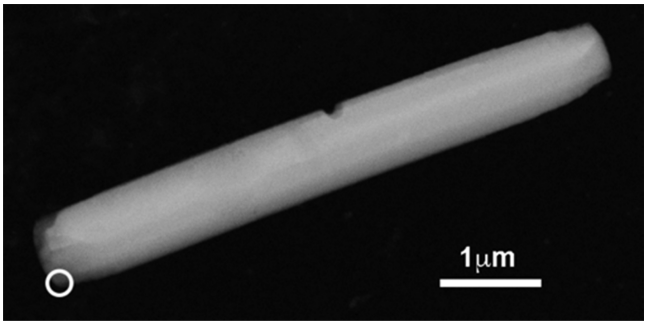

Figure 2. STEM image of a RAM crystal, with the marked area showing the place where 3D PEDT data were collected.

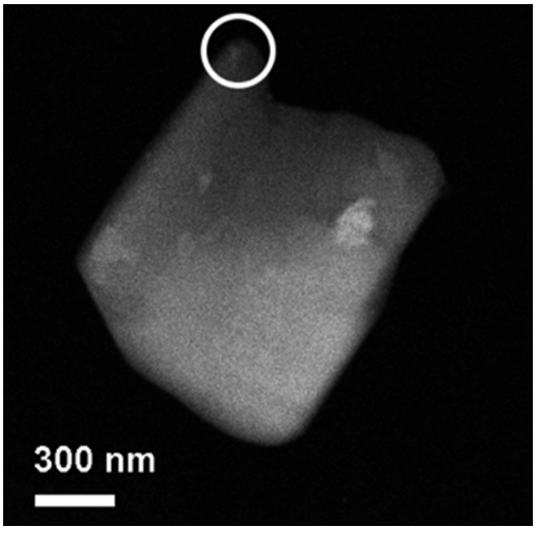

Figure 3. STEM image of a TOL crystal, with the marked area showing the place where 3D ED tomography data were collected.

PEDT data from three TOL crystals (Figure 3) were instead acquired in steady steps of 1° after the sample was cooled to liquid N_2 temperature. After each pattern acquisition, the crystal position was tracked in STEM mode in order to further reduce the electron dose on the sample. The precession angle was kept at 1°. The acquisition protocol is similar to the one described for previous PEDT experiments on very beam-sensitive materials.[20,22]

During the acquisition, we took care that high-angle reflections were still visible for the entire tilt range. The reduction of the effective resolution is in fact a well-known indication of ongoing beam damage[31] that would otherwise introduce random noise in the data set. The data were collected in STEM mode under low-dose conditions, so no obvious beam damage of the crystals was observed. However, merging of multiple data sets was necessary because the sample thickness appeared to be a serious issue at high tilt angle and often obliged

DOI: 10.1021/acs.oprd.8b00149
Org. Process Res. Dev. 2018, 22, 1365−1372

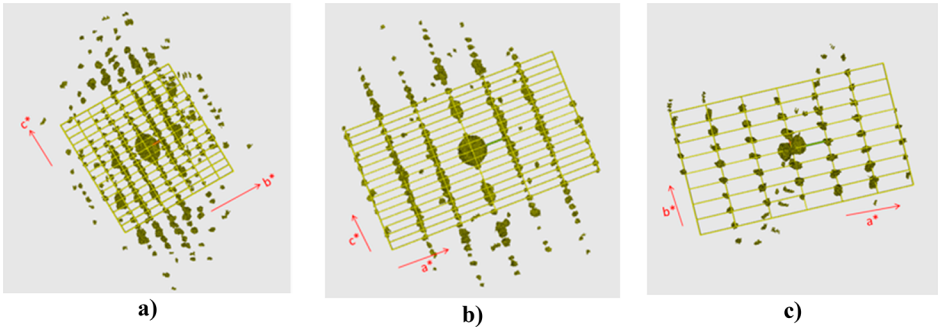

Figure 4. Projections of the 3D reconstructed diffraction volume from PEDT data for RAM: (a) a^* [100] projection; (b) b^* [010] projection; (c) c^* [001] projection. The grids show the projections of the unit cell.

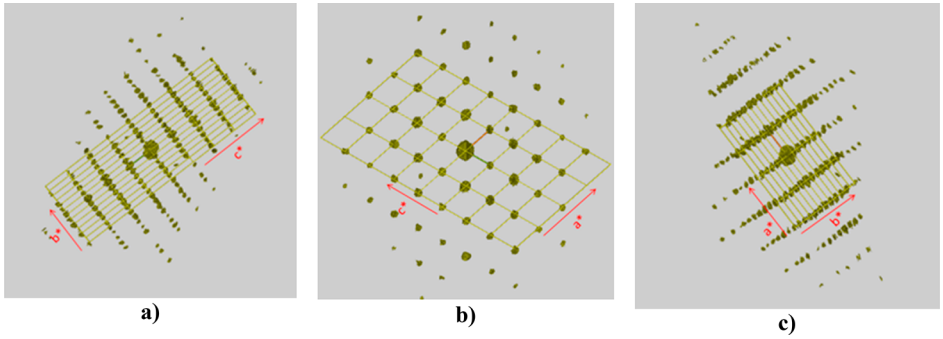

Figure 5. Projections of the 3D reconstructed diffraction volume from PEDT data for TOL: (a) a^* [100] projection; (b) b^* [010] projection; (c) c^* [001] projection. The grids show the projections of the unit cell.

us to interrupt data collection. The data were later processed using ADT3D software for unit cell determination and reflection intensity integration.[39] The software takes the maximum intensity recorded for each reflection.

2.3. X-ray Crystallography. Single-crystal diffraction data were collected on an Oxford Diffraction SuperNova dual-wavelength diffractometer with operating mirror monochromatized Cu Kα radiation mode (λ = 1.5418 Å).[41] X-ray data collection was monitored, and all of the data were corrected for Lorentzian, polarization, and absorption effects using the CrysAlisPro program.[42] The OLEX2 program was used for crystal structure solution and refinement.[43] SHELXS97[44] was used for structure solution, and SHELXL[45] was used for full-matrix least-squares refinement on F^2.

3. RESULTS AND DISCUSSION

3.1. Electron Diffraction Data Processing. For the RAM sample, an orthorhombic unit cell with a = 4.99 Å, b = 11.92 Å, and c = 22.95 Å (Table 1) was calculated by averaging of four indexed PEDT data sets. This unit cell is consistent with the one obtained from single-crystal X-ray diffraction data collected at room temperature (a = 5.0450 Å, b = 12.4178 Å, and c = 23.187 Å). Assuming orthorhombic Laue symmetry (mmm), R_{int} of the merged PEDT data was 24.40%. On the basis of the PEDT intensity statistics, the SIR2014 software[46] automatically suggested the orthorhombic space group $P2_12_12_1$ (FOM 0.376), which is consistent with the one obtained from the single-crystal X-ray diffraction data. In order to increase the overall data completeness and reduce the effect of random noise, data from individual nanocrystals were eventually merged into a unique *hkl* file. In this way, 88.2% of the independent reflections up to 1 Å resolution were included in the data set. Unit cell projections along the three main crystallographic axes are shown in Figure 4.

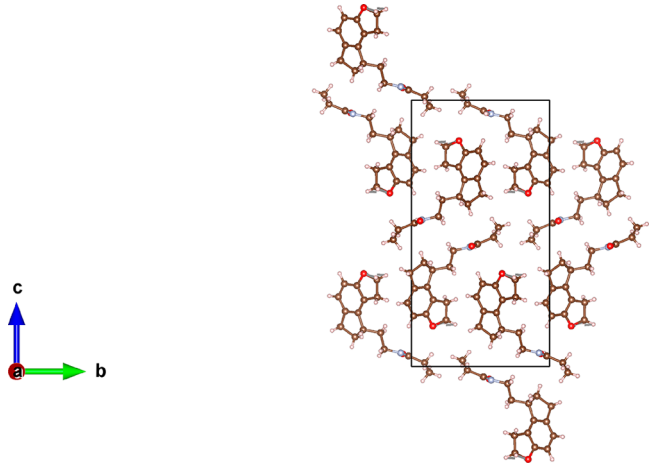

Figure 6. RAM crystal structure solved by SA on the basis of 3D PEDT data (atom colors: C, brown; O, red; N, blue; H, white).

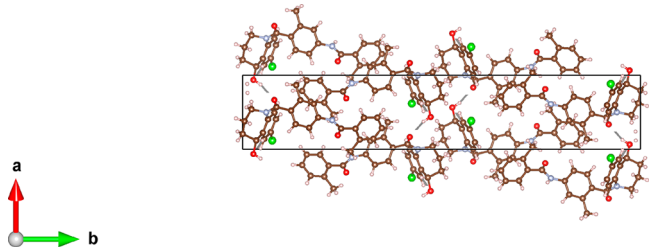

Figure 7. TOL crystal structure solved by SA on the basis of 3D PEDT data (atom colors: C, brown; O, red; N, blue; Cl, green; H, white).

DOI: 10.1021/acs.oprd.8b00149
Org. Process Res. Dev. 2018, 22, 1365−1372

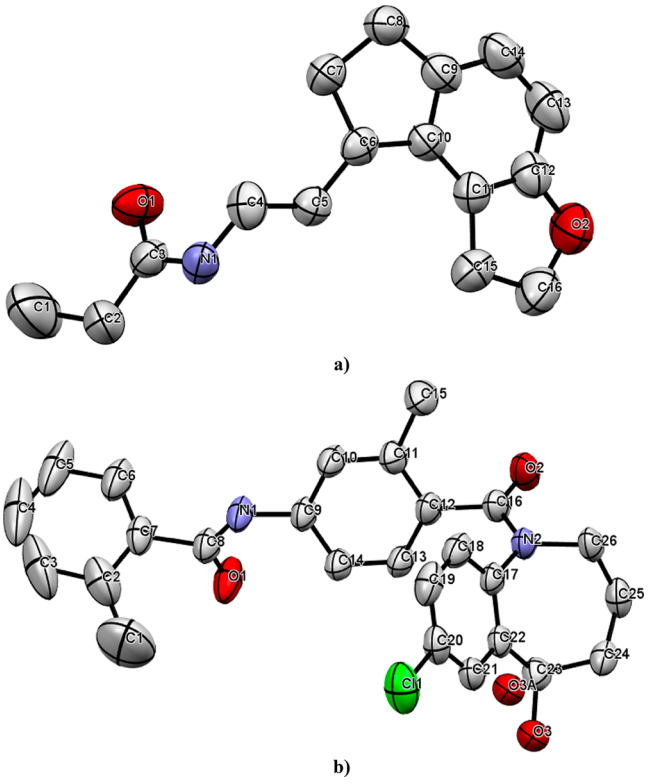

Figure 8. ORTEP drawings and numbering schemes of (a) RAM and (b) TOL. H atoms have been omitted for clarity.

Table 2. Important Intermolecular Hydrogen Bonds in the RAM and TOL Crystal Structures

structure	D−H···A	d_{D-H} (Å)	$d_{H\cdots A}$ (Å)	$d_{D\cdots A}$ (Å)	D−H···A angle (deg)
RAM	N1−H1···O1	0.86	2.09	2.882(4)	153
TOL	N1−H1···O1	0.86	2.04	2.897(5)	173
	O3−H3A···O2	0.82	2.00	2.781(5)	159

Table 3. Overlay Parameters for RAM and TOL Molecules in the PEDT and X-ray Structures

	RMSD (Å)	max(D) (Å)
RAM	0.12	0.28
TOL	0.09	0.32

For the TOL sample, an average monoclinic unit cell with a = 7.52 Å, b = 38.53 Å, c = 8.44 Å, and β = 107.82° was calculated from the three PEDT data sets acquired at liquid N_2 temperature. This unit cell is consistent with the one obtained from single-crystal X-ray diffraction data collected at room temperature (a = 7.627 Å, b = 38.007 Å, c = 8.5629 Å, and β = 108.118°). Assuming monoclinic Laue symmetry ($2/m$), R_{int} of the merged PEDT data was 16.55%. The SIR2014 software automatically suggested the monoclinic space group $P2_1/n$ (FOM 0.687). As for RAM, intensities from the individual data sets were merged, increasing the data completeness up to 64.35% (at a resolution of 1.2 Å). Unit cell projections along the three main crystallographic axes are shown in Figure 5.

One can remark that both the TOL and RAM merged data sets had R_{int} values in the 20−30% range that is usually encountered in inorganic, not-problematic structures, while values above 30% would be expected for beam-sensitive or defective materials.[15]

3.2. Structure Solution from the PEDT Data. Structure solution was performed by simulated annealing (SA) as implemented in the SIR2014 software[46] (which includes scattering factors for electrons), using as input the merged PEDT data sets for RAM and TOL. Despite the acceptable R_{int} values of both merged data sets, attempts at ab initio solution of the crystal structures were not successful.

SA is a global optimization method that is analogous to searching for a low-energy state in a physical system by annealing it.[47,48] SA requires an a priori model of the molecule. Interatomic connectivity and distances and rigid parts of the molecules (like phenyl rings) are not changed during the structure determination process. Conversely, global shift and rotation of the molecule (six global parameters) and nonconstrained torsion angles (internal degrees of freedom of the molecule) are free to change until an optimal convergence between the observed and calculated reflection intensities is obtained. The a priori molecular structure is normally obtained by IR or NMR measurements or from similar molecular structures deposited in crystal structure databases like CSD,[49] ICDD,[50] or COD.[51] For both RAM and TOL, initial molecules were available from the literature.[52] They are shown in Figure 1a and Figure 1b, respectively.

The cost function (CF) parameter that has to be minimized during the SA process is analogous to the energy of the system in the annealing process and is related to the R factor by eq 1:

$$\mathrm{CF} = \sqrt{\sum_h (F_h^{obs} - kF_h^{calc})^2 / \sum_h (F_h^{obs})^2} \quad (1)$$

where k is the scale factor and F is the structure factor. SIR2014 uses the "hybrid big bang−big crunch" (HBB-BC) optimization algorithm, performing a search in the sample configuration space in a uniform manner at some high-temperature/high-energy

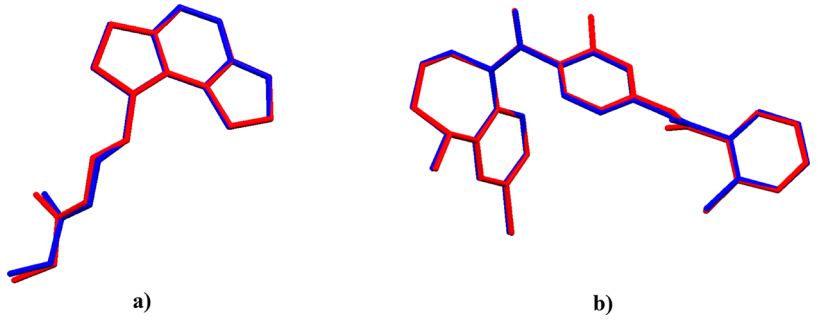

Figure 9. Overlays of the (a) RAM and (b) TOL molecules from PEDT (blue) and single-crystal X-ray (red) structure determinations.

DOI: 10.1021/acs.oprd.8b00149
Org. Process Res. Dev. 2018, 22, 1365−1372

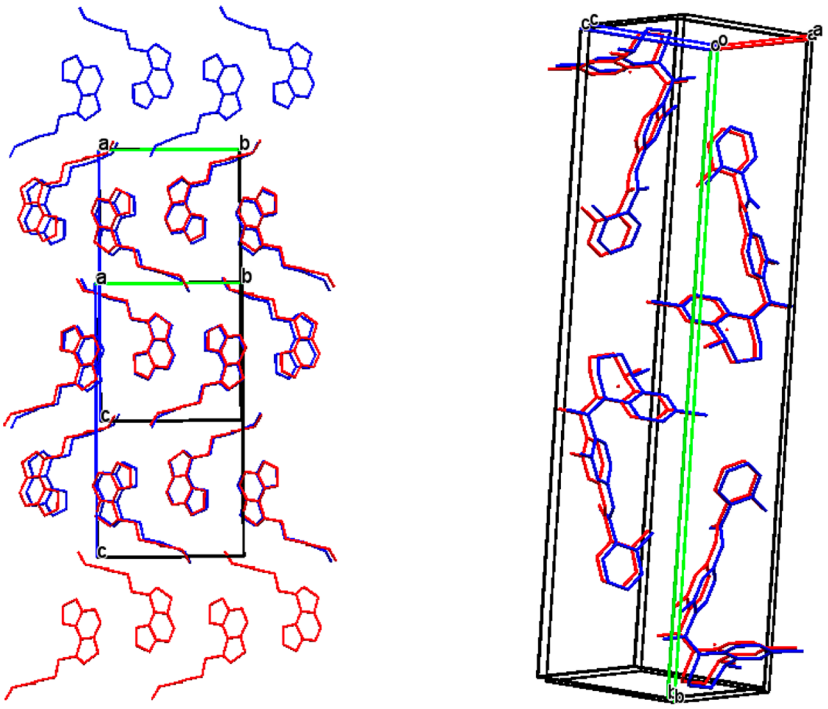

Figure 10. Full structure overlays of the (a) RAM and (b) TOL structures determined on the basis of PEDT (blue) and single-crystal X-ray (red) data.

state.[53,54] During SA structure solution, the same loop is repeated as the temperature/energy is lowered until the system is relaxed at the lowest possible stable energy (satisfactory solution). The success of SA deeply relies on the accuracy of the chemical information and the correctness of the initial molecular fragment. At the end of the process, it is possible to recognize and screen the correct SA solution considering the correctness of the intermolecular connectivity and bonding.

For the RAM structure, SA required the determination of 11 parameters: six global parameters (shift and rotation of the molecule) and five torsion angles (internal degrees of freedom). For structure solution, 340 PEDT reflections with up to 1.4 Å resolution were used. The random starting temperature of SA gave an initial CF of 103.888. After the SA run, the best crystal−chemical correct model gave a CF of 42.760. The correct model found after SA for RAM is shown in Figure 6. The hydrogen atom positions were fixed in the final structure considering the geometry of the terminal atom.

For the TOL structure, SA also required the determination of 11 parameters. Structure solution was achieved using 1028 PEDT reflections with up to 1.2 Å resolution. The random starting temperature of SA gave an initial CF of 95.202. After SA solution, the best crystal−chemical correct model gave a CF of 41.52. The correct model found after SA for TOL is shown in Figure 7. The hydrogen atom positions were also in this case fixed in the final structure considering the geometry of the terminal atom.

In both cases, the quality of the RAM and TOL electron diffraction data sets did not allow for least-squares refinement without restraints and constraints. Therefore, we used X-ray crystallography to validate the structure solutions obtained by electron diffraction (Table 3 and Figures 9 and 10). Further investigation of the refinement of electron diffraction data will be the subject of a future study.

3.3. Analysis of the Crystal Structures. The crystallographic data for the RAM and TOL drug substances determined by PEDT and X-ray crystallography are presented in Table 1. The ORTEP drawings and numbering schemes of the RAM and TOL molecules in the determined X-ray crystal structures are shown in Figure 8.

The RAM structure is characterized by crystal packing with no residual solvent-accessible voids (packing index of 65.5%, typical for stable molecular crystals). The RAM molecules are hydrogen-bonded in a 1D infinite chain along the *a* axis (Figure S2 in the Supporting Information).

In the X-ray structure of TOL, positional disorder is observed at the O3 atom (the occupancy of the O3 atoms is 84:16; see Figure 8b). Also, there is 3.6% potential solvent volume per unit cell volume (Figure S1), indicating that small solvent molecules might be incorporated in the structure voids. Despite this, the crystal packing is stabilized by intermolecular hydrogen bonds that create infinite 1D chains and circuits and an infinite 2D network of the TOL molecules (Table 2 and Figure S3).

Generally, it is very difficult to evidence the disorder from electron crystallography by using kinematically refined PED data.[57] Recent developments in the field showed the potential of dynamical refinement in the localization of hydrogen atoms,[58] suggesting that disorder might be evidenced by this technique. However, the quality of the RAM and TOL electron diffraction data sets did not allow for an ab initio structure solution and consequently for an attempt at dynamical refinement.

3.4. Molecule and Structure Overlays. The similarity between the crystal structures obtained from PEDT and X-ray diffraction was quantified using molecule and structure overlay calculations as implemented in the Mercury software.[38] Pairs of atoms from the two crystal structures were used to calculate the root-mean-square deviation (RMSD) and the maximum distance between two equivalent atoms in the molecule overlay (max(D)) (Table 3).

DOI: 10.1021/acs.oprd.8b00149
Org. Process Res. Dev. 2018, 22, 1365−1372

Both the molecular conformations of the RAM and TOL molecules and their crystal packings are highly similar in the PEDT and X-ray structures (Figure 9). In the case of the full structure overlays (Figure 10), small shifts of the molecules in the unit cells are mostly due to the differences between the unit cells determined from PEDT and X-ray diffraction. The errors in unit cell parameter determination by PEDT are estimated to be about 1−3%.[55] For the present experiments, only the *b* axis of RAM shows a discrepancy higher than 1.5%. In any event, this does not affect the accuracy of the molecular configuration.

4. CONCLUSIONS

The unknown structures of two complex pharmaceutical compounds were solved by simulated annealing (SA) using diffraction data collected from nanosized crystals by the novel method 3D precession electron diffraction tomography (PEDT).

Two different acquisition protocols designed for beam-sensitive materials, respectively based on sample cooling and ultrafast continuous data acquisition, can be adopted and deliver comparable results. Notably, SA is a robust protocol for structure solution that can be used to determine the atomic structure also for nonoptimal data when standard direct methods fail. Moreover, no least-squares refinement was necessary for the crystal structures solved using PEDT data in order to achieve a good match with the X-ray structures, thereby validating the developed workflow for data acquisition and structure solution with electron diffraction.

Our results emphasize the potential of the PEDT technique in providing accurate crystal structures of pharmaceutical nanocrystals that will suffice for most practical applications when no larger crystals can be grown. It can be envisaged that PEDT may identify small amounts of newly appearing polymorphs in batches prone to polymorphic transformations.

■ ASSOCIATED CONTENT

Supporting Information

The Supporting Information is available free of charge on the ACS Publications website at DOI: 10.1021/acs.oprd.8b00149.

Solvent screening experiments and hydrogen bonding networks in the RAM and TOL crystal structures (PDF)
X-ray crystallographic data for RAM (CIF)
X-ray crystallographic data for TOL (CIF)
Electron crystallographic data for RAM (CIF)
Electron crystallographic data for TOL (CIF)

■ AUTHOR INFORMATION

Corresponding Author

*E-mail: mihaela.pop@teracrystal.com. Tel/Fax: +40 364 439995.

ORCID

Mauro Gemmi: 0000-0001-9542-3783
Mihaela M. Pop: 0000-0002-5555-6562

Notes

The authors declare no competing financial interest.

■ ACKNOWLEDGMENTS

From the National Institute for R&D of Isotopic and Molecular Technologies, Cluj-Napoca, Romania, we thank F. A. Martin and M. Miclaus for help with the crystal growth experiments. Support from the Romanian National Authority for Scientific Research (Project POSCCE ID536) is acknowledged for the X-ray single-crystal work.

■ REFERENCES

(1) Lee, A. Y.; Erdemir, D.; Myerson, A. S. Crystal polymorphism in chemical process development. *Annu. Rev. Chem. Biomol. Eng.* **2011**, *2*, 259−280.

(2) Borodi, G.; Pop, M. M.; Onija, O.; Filip, X. Distinct Disordered Forms of Promethazine Hydrochloride: A Case of Intergrowth of Polymorphic Domains? *Cryst. Growth Des.* **2012**, *12*, 5846−5851.

(3) Skorepova, E.; Cejka, J.; Husak, M.; Eigner, V. A.; Rohlicek, J.; Sturc, A.; Kratochvil, B. Trospium Chloride: Unusual Example of Polymorphism Based on Structure Disorder. *Cryst. Growth Des.* **2013**, *13*, 5193−5203.

(4) Price, L. S.; McMahon, J. A.; Lingireddy, S. R.; Lau, S.-F.; Diseroad, B. A.; Price, S. L.; Reutzel-Edens, S. M. A molecular picture of the problems in ensuring structural purity of tazofelone. *J. Mol. Struct.* **2014**, *1078*, 26−42.

(5) Desiraju, G. R. Chemical crystallography and crystal engineering. *IUCrJ* **2014**, *1*, 380−381.

(6) Florence, A.; Johnston, A.; Fernandes, P.; Shankland, K.; Stevens, H. N. E.; Osmundsen, S.; Mullen, A. B. Powder study of hydrochlorothiazide form II. *Acta Crystallogr., Sect. E: Struct. Rep. Online* **2005**, *61*, o2798−o2800.

(7) Harris, K. D. M. Structure solution from powder X-ray diffraction data by genetic algorithm techniques, applied to organic materials generated as polycrystalline products from solid state processes. *Mater. Manuf. Processes* **2009**, *24*, 293−302.

(8) Miclaus, M.; Grosu, I. G.; Filip, X.; Tripon, C.; Filip, C. Optimizing structure determination from powders of crystalline organic solids with high molecular flexibility: the case of lisinopril dehydrate. *CrystEngComm* **2014**, *16*, 299−303.

(9) Luedeker, D.; Gossmann, R.; Langer, K.; Brunklaus, G. Crystal Engineering of Pharmaceutical Co-crystals: "NMR Crystallography" of Niclosamide Co-crystals. *Cryst. Growth Des.* **2016**, *16*, 3087−3100.

(10) David, W. I. F.; Shankland, K. Structure determination from powder diffraction data. *Acta Crystallogr., Sect. A: Found. Crystallogr.* **2008**, *64*, 52−64 and references therein.

(11) Dorset, D. L. *Structural Electron Crystallography*; Plenum Press: New York, 1995.

(12) Kolb, U.; Gorelik, T. E.; Kubel, C.; Otten, M. T.; Hubert, D. Towards automated diffraction tomography: Part I—Data acquisition. *Ultramicroscopy* **2007**, *107*, 507−513.

(13) Kolb, U.; Gorelik, T. E.; Otten, M. T. Towards automated diffraction tomography. Part II—Cell parameter determination. *Ultramicroscopy* **2008**, *108*, 763−772.

(14) Gemmi, M.; La Placa, M. G. I.; Galanis, A.; Rauch, E. F.; Nicolopoulos, S. Fast electron diffraction tomography. *J. Appl. Crystallogr.* **2015**, *48*, 718−727.

(15) Mugnaioli, E.; Kolb, U. Structure characterization of nanocrystalline porous materials by tomographic electron diffraction. *Z. Kristallogr. - Cryst. Mater.* **2015**, *230*, 271−288.

(16) Vincent, R.; Midgley, P. A. Double conical beam-rocking system for measurement of integrated electron diffraction intensities. *Ultramicroscopy* **1994**, *53*, 271−282.

(17) Proceedings of the Electron Crystallography School 2005 (ELCRYST 2005): New Frontiers in Electron Crystallography: *Ultramicroscopy* **2007**, *107*, 431−558.

(18) Mugnaioli, E.; Gorelik, T.; Kolb, T. "Ab initio" structure solution from electron diffraction data obtained by a combination of automated diffraction tomography and precession technique. *Ultramicroscopy* **2009**, *109*, 758−765.

(19) Gorelik, T. E.; Stewart, A. A.; Kolb, U. Structure solution with automated electron diffraction tomography data: different instrumental approaches. *J. Microsc.* **2011**, *244*, 325−331.

(20) Jiang, J.; Jorda, J. L.; Yu, J.; Baumes, L. A.; Mugnaioli, E.; Diaz-Cabanas, M. J.; Kolb, U.; Corma, A. Synthesis and Structure Determination of the Hierarchical Meso-Microporous Zeolite ITQ-43. *Science* **2011**, *333*, 1131−1134.

DOI: 10.1021/acs.oprd.8b00149
Org. Process Res. Dev. 2018, 22, 1365−1372

(21) Simancas, J.; Simancas, R.; Bereciartua, P. J.; Jorda, J. L.; Rey, F.; Corma, A.; Nicolopoulos, S.; Das, P. P.; Gemmi, M.; Mugnaioli, E. Ultrafast Electron Diffraction Tomography for Structure Determination of the New Zeolite ITQ-58. *J. Am. Chem. Soc.* **2016**, *138*, 10116−10119.
(22) Feyand, M.; Mugnaioli, E.; Vermoortele, F.; Bueken, B.; Dieterich, J. M.; Reimer, T.; Kolb, U.; de Vos, D.; Stock, N. Automated Diffraction Tomography for the Structure Elucidation of Twinned, Sub-micrometer Crystals of a Highly Porous, Catalytically Active Bismuth Metal−Organic Framework. *Angew. Chem.* **2012**, *124*, 10519−10522.
(23) Wang, Y.; Takki, S.; Cheung, O.; Xu, H.; Wan, W.; Öhrström, L.; Inge, A. K. Elucidation of the elusive structure and formula of the active pharmaceutical ingredient bismuth subgallate by continuous rotation electron diffraction. *Chem. Commun.* **2017**, *53*, 7018−7021.
(24) Rozhdestvenskaya, I.; Mugnaioli, E.; Czank, M.; Depmeier, W.; Kolb, U.; Reinholdt, A.; Weirich, T. The structure of charoite, $(K,Sr,Ba,Mn)_{15-16}(Ca,Na)_{32}[(Si_{70}(O,OH)_{180})](OH,F)_{4.0}\cdot nH_2O$, solved by conventional and automated electron diffraction. *Mineral. Mag.* **2010**, *74*, 159−177.
(25) Gemmi, M.; Fischer, J. K.; Merlini, M.; Poli, S.; Fumagalli, P.; Mugnaioli, E.; Kolb, U. A new hydrous Al-bearing pyroxene as a water carrier in subduction zones. *Earth Planet. Sci. Lett.* **2011**, *310*, 422−428.
(26) Sarakinou, E.; Mugnaioli, E.; Lioutas, C. B.; Vouroutzis, N.; Frangis, N.; Kolb, U.; Nikolopoulos, S. Structure characterization of hard materials by precession electron diffraction and automatic diffraction tomography: 6H−SiC semiconductor and $Ni_{1+x}Te_1$ embedded nanodomains. *Semicond. Sci. Technol.* **2012**, *27*, 105003.
(27) Samuha, S.; Mugnaioli, E.; Grushko, B.; Kolb, K.; Meshi, L. Atomic structure solution of the complex quasicrystal approximant $Al_{77}Rh_{15}Ru_8$ from electron diffraction data. *Acta Crystallogr., Sect. B: Struct. Sci., Cryst. Eng. Mater.* **2014**, *70*, 999−1005.
(28) Andrusenko, I.; Krysiak, Y.; Mugnaioli, E.; Gorelik, T. E.; Nihtianova, D.; Kolb, U. Structural insights into $M_2O-Al_2O_3-WO_3$ (M = Na, K) system by electron diffraction tomography. *Acta Crystallogr., Sect. B: Struct. Sci., Cryst. Eng. Mater.* **2015**, *71*, 349−357.
(29) Mugnaioli, E.; Gemmi, M.; Merlini, M.; Gregorkiewitz, M. $(Na,\square)_5[MnO_2]_{13}$ nanorods: a new tunnel structure for electrode materials determined ab initio and refined through a combination of electron and synchrotron diffraction data. *Acta Crystallogr., Sect. B: Struct. Sci., Cryst. Eng. Mater.* **2016**, *72*, 893−903.
(30) Gorelik, T.; Matveeva, G.; Schleuß, T.; Kilbinger, A. F. M.; van de Streek, J.; Bohle, A.; Brunklaus, G.; Kolb, U. H-bonding schemes of di- and tri-*p*-benzamides assessed by a combination of electron diffraction, X-ray powder diffraction and solid-state NMR. *CrystEngComm* **2010**, *12*, 1824−1832.
(31) Kolb, U.; Gorelik, T. E.; Mugnaioli, E.; Stewart, A. Structural Characterization of Organics Using Manual and Automated Electron Diffraction. *Polym. Rev.* **2010**, *50*, 385−409.
(32) van Genderen, E.; Clabbers, M. T. B; Das, P. P.; Stewart, A.; Nederlof, I.; Barentsen, K. C.; Portillo, Q.; Pannu, N. S.; Nicolopoulos, S.; Gruene, T.; Abrahams, J. P. Ab initio structure determination of nanocrystals of organic pharmaceutical compounds by electron diffraction at room temperature using a Timepix quantum area direct electron detector. *Acta Crystallogr., Sect. A: Found. Adv.* **2016**, *72*, 236−242.
(33) Neubauer, D. N. A review of ramelteon in the treatment of sleep disorders. *Neuropsychiatr Dis Treat.* **2008**, *4*, 69−79.
(34) Osanai, K.; Kobayashi, Y.; Otsu, M.; Izawa, T.; Sakai, K.; Iwashita, M. Ramelteon, a selective MT1/MT2 receptor agonist, suppresses the proliferation and invasiveness of endometrial cancer cells. *Hum. Cell* **2017**, *30*, 209−215.
(35) Takeda Global Research and Development Center. Chemistry Review, NDA 21-782, 2005.
(36) Otsuka Pharmaceutical Co. NDA No. 022275, 2009.
(37) Allen, F. H. The Cambridge Structural Database: a quarter of a million crystal structures and rising. *Acta Crystallogr., Sect. B: Struct. Sci.* **2002**, *58*, 380−388.
(38) *Mercury: Software for Crystal Structure Visualization, Exploration, and Analysis*, version 3.3; Cambridge Crystallographic Data Centre: Cambridge, U.K., 2013.
(39) NanoMEGAS SPRL (Brussels, Belgium). www.nanomegas.com.
(40) Amsterdam Scientific Instruments (Amsterdam, The Netherlands). www.amscins.com.
(41) Rigaku Oxford Diffraction. http://www.rigaku.com/en/rigakuoxford.
(42) *CrysAlis PRO*; Agilent Technologies: Yarnton, U.K., 2010.
(43) Dolomanov, O. V.; Bourhis, L. J.; Gildea, R. J.; Howard, J. A. K.; Puschmann, H. OLEX2: a complete structure solution refinement and analysis program. *J. Appl. Crystallogr.* **2009**, *42*, 339−341.
(44) Sheldrick, G. M. *SHELXS97*; University of Göttingen: Göttingen, Germany, 1990.
(45) Sheldrick, G. M. A short history of SHELX. *Acta Crystallogr., Sect. A: Found. Crystallogr.* **2008**, *64*, 112−122.
(46) Burla, M. C.; Caliandro, R.; Carrozzini, B.; Cascarano, G. L.; Cuocci, C.; Giacovazzo, C.; Mallamo, M.; Mazzone, A.; Polidori, G. Crystal structure determination and refinement via SIR2014. *J. Appl. Crystallogr.* **2015**, *48*, 306−309.
(47) David, W. I. F.; Shankland, K.; Shankland, N. Routine determination of molecular crystal structures from powder diffraction data. *Chem. Commun.* **1998**, 931−932.
(48) Pagola, S.; Stephens, P. W.; Bohle, D. S.; Kosar, A. D.; Madsen, S. K. The structure of malaria pigment β-haematin. *Nature* **2000**, *404*, 307−310.
(49) Groom, C. R.; Bruno, I. J.; Lightfoot, M. P.; Ward, S. C. The Cambridge Structural Database. *Acta Crystallogr., Sect. B: Struct. Sci., Cryst. Eng. Mater.* **2016**, *72*, 171−179.
(50) Faber, J. *J. Ceram. Soc. Jpn.* **2004**, *112*, S1434−S1438.
(51) Grazulis, S.; Chateigner, D.; Downs, R. T.; Yokochi, A. T.; Quiros, M.; Lutterotti, L.; Manakova, E.; Butkus, J.; Moeck, P.; Le Bail, A. Crystallography Open Database - an open-access collection of crystal structures. *J. Appl. Crystallogr.* **2009**, *42*, 726−729.
(52) Kim, S.; Thiessen, P. A.; Bolton, E. E.; Chen, J.; Fu, G.; Gindulyte, A.; Han, L.; He, J.; He, S.; Shoemaker, B. A.; Wang, J.; Yu, B.; Zhang, J.; Bryant, S. H. PubChem Substance and Compound databases. *Nucleic Acids Res.* **2016**, *44*, D1202−D1213.
(53) Favre-Nicolin, V.; Cerný, R. FOX, 'free objects for crystallography': a modular approach to ab initio structure determination from powder diffraction. *J. Appl. Crystallogr.* **2002**, *35*, 734−743.
(54) Altomare, A.; Corriero, N.; Cuocci, C.; Moliterni, A.; Rizzi, R. The hybrid big bang-big crunch method for solving crystal structure from powder diffraction data. *J. Appl. Crystallogr.* **2013**, *46*, 779−787.
(55) Kolb, U.; Mugnaioli, E.; Gorelik, T. E. Automated electron diffraction tomography − a new tool for nano crystal structure analysis. *Cryst. Res. Technol.* **2011**, *46*, 542−554.
(56) Yonekura, K.; Maki-Yonekura, S.; Namba, K. *Biophys. J.* **2002**, *82* (5), 2784−97.
(57) Palatinus, L.; Corrêa, C. A.; Steciuk, G.; Jacob, D.; Roussel, P.; Boullay, P.; Klementová, M.; Gemmi, M.; Kopeček, J.; Domeneghetti, M. C.; Cámara, F.; Petříček, V. *Acta Crystallogr., Sect. B: Struct. Sci., Cryst. Eng. Mater.* **2015**, *71*, 740−51.
(58) Palatinus, L.; Brazda, P.; Boullay, P.; Perez, O.; Klementová, M.; Petit, S.; Eigner, V.; Zaarour, M.; Mintova, S. *Science* **2017**, *355*, 166−169.

DOI: 10.1021/acs.oprd.8b00149
Org. Process Res. Dev. 2018, 22, 1365−1372